

An Analytical Approximation for the Pull-Out Frequency of a PLL Employing a Sinusoidal Phase Detector

Abu-Sayeed Huque and John Stensby

The pull-out frequency of a second-order phase lock loop (PLL) is an important parameter that quantifies the loop's ability to stay frequency locked under abrupt changes in the reference input frequency. In most cases, this must be determined numerically or approximated using asymptotic techniques, both of which require special knowledge, skills, and tools. An approximating formula is derived analytically for computing the pull-out frequency for a second-order Type II PLL that employs a sinusoidal characteristic phase detector. The pull-out frequency of such PLLs can be easily approximated to satisfactory accuracy with this formula using a modern scientific calculator.

Keywords: Phase lock loop (PLL), phase detector (PD), voltage controlled oscillator (VCO), hyperbolic equilibrium point, phase plane, phase portrait, saddle point, focus, separatrix.

I. Introduction

A PLL is an essential component in the synchronization block in many data communication systems. System model analysis is a standard practice in the PLL design effort, just as it is in the design processes of many other branches of engineering. Among the existing models, the second-order PLL models remain the most useful for most applications. Even in the second-order PLL models, there are two kinds, known as the Type I and Type II models. Due to the simplicity of behavioral analysis combined with adequately satisfactory performance for most applications, Type II models stand out as the starting point for almost all PLL design efforts. A sinusoidal phase detector (PD) in the PLL system architecture has been the most common type of PD, though other kinds, such as triangular, tanlog, and so on, are not rare in modern PLLs.

The pull-out frequency is a very important parameter for a second-order Type II PLL. It is a measure of the loop's ability to relock in the same cycle, when an abrupt change in frequency is experienced at the input reference and/or at the output of the voltage controlled oscillator (VCO) under a locked condition. In many systems, such as synchronous block data transfer and training pulse retrieval, loss of cycle(s), also known as the cycle-slip, cannot be tolerated between the loss of lock and the relocking back to the reference frequency by the PLL.

In the literature, there exists an empirical formula, deduced by Viterbi, to approximate the pull-out frequency of a second-order Type II PLL containing a sinusoidal PD [1], [2]. However, there have not been any known analytical approaches to derive either an exact or an approximating formula to calculate the same. This paper proposes an analytically derived formula, to approximate the *pull-out*

Manuscript received Mar. 11, 2012; revised Sept. 20, 2012; accepted Oct. 4, 2012.

Abu-Sayeed Huque (ahuque@ut.edu.sa) was with the Department of Math & Computer Science, Oakwood University, Alabama, USA, and is now with the Department of Electrical Engineering, University of Tabuk, Saudi Arabia.

John Stensby (stensby@eng.uah.edu) is with the Department of Electrical and Computer Engineering, University of Alabama Huntsville, Huntsville, USA.

<http://dx.doi.org/10.4218/etrij.13.0112.0166>

frequency of a second-order Type II PLL that employs a sinusoidal PD, which outperforms the existing empirical formula for most parts of the practical range of the loop parameter(s). The authors have also derived an exact formula to calculate the same parameter for the loops employing the triangular PD [3].

Section II depicts a block diagram and the associated system model of a second-order Type II PLL employing a sinusoidal PD. It then continues with the derivation of the system equation for said PLL.

Section III starts with finding the equilibrium points and their nature, which determine the local behavior of the system around the equilibrium points. Since the system is nonlinear, it is not surprising that the solution may not be found in a closed form. Therefore, a standard technique in analyzing second-order nonlinear systems, known as the *phase portrait*, is used to analyze the dynamical behavior of the systems.

Section IV introduces the definition of the pull-out frequency (Ω_{po}) in light of the phase portrait and also briefly discusses the importance of this parameter in real applications.

Section V contains an analytical approach to derive an approximating formula to calculate Ω_{po} for a second-order PLL containing a sinusoidal PD.

Section VI validates the derived formula against the numerically calculated results. It also compares the pull-out frequency approximated by this formula with the approximation produced by the existing empirical formula.

Section VII highlights a few applications in which the pull-out frequency is directly used. Finally, some light is shed on how the derived formula outperforms the existing empirical formula.

II. System Model for Second-Order Type II PLL Employing Sinusoidal PD

A block diagram for a second-order Type II PLL containing a sinusoidal PD, implemented commonly as an analog multiplier, is shown in Fig. 1. Here, the sinusoidal reference input (v_{ref}) and the VCO output (v_{vco}) are fed to the PD.

In Fig. 1, θ_i and θ_v are the instantaneous phase of the reference input and that of the VCO output signal, respectively, where ω_i and ω_0 are the frequency of the reference input and center (quiescent) frequency of the VCO, respectively. The difference between the two input phases to the PD is known as the phase error, which is defined as

$$\phi(t) = \theta_i(t) - \theta_v(t). \quad (1)$$

The PD produces a signal $g(\phi)$, which is a function of the phase error, while for sinusoidal PD it is given as

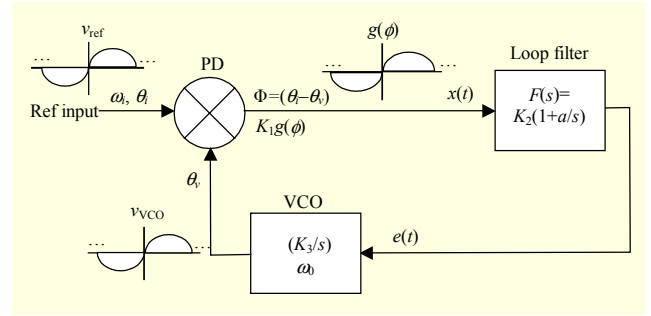


Fig. 1. System model of second-order Type II PLL employing sinusoidal PD.

$$g(\phi) = \sin \phi. \quad (2)$$

Thus, the input signal to the loop filter can be described as

$$x(t) = K_1 g(\phi), \quad (3)$$

where K_1 is known as the PD gain. For a second-order Type II PLL, the transfer function of the loop filter is defined as

$$F(s) = K_2 \left(1 + \frac{a}{s} \right), \quad (4)$$

where K_2 is known as the loop filter gain and the positive constant a ($a > 0$ in practice) is known as the integrator gain. By taking the inverse Laplace transform of (4), the transfer function can be represented in the time domain, assuming zero initial condition, $e(0) = 0$, as

$$\frac{d}{dt} e(t) = K_2 \left(\frac{d}{dt} + a \right) x(t). \quad (5)$$

Here, $e(t)$, the output of the loop filter feeding into the VCO, is commonly known as the error signal or the control voltage. A standard way to mathematically model a VCO is

$$\frac{d\theta_v}{dt} = \omega_0 + K_3 e(t), \quad (6)$$

where K_3 is called the VCO gain [2]. This implies that the frequency of the VCO is tuned around its center frequency (ω_0) by the control voltage $e(t)$. The derivation of the overall system model can be greatly simplified by redefining two new relative phase terms as

$$\theta_1 = \theta_i - \omega_0 t = (\omega_i - \omega_0)t = \omega_\Delta t, \quad (7)$$

$$\theta_2 = \theta_v - \omega_0 t. \quad (8)$$

Here, θ_1 and θ_2 are the relative instantaneous phase of the reference input and that of the VCO output signal. The difference between the reference frequency (ω_i) and the center frequency of the VCO (ω_0) is known as the detuning parameter (ω_Δ) in the PLL literature. Thus, the phase error at the output of

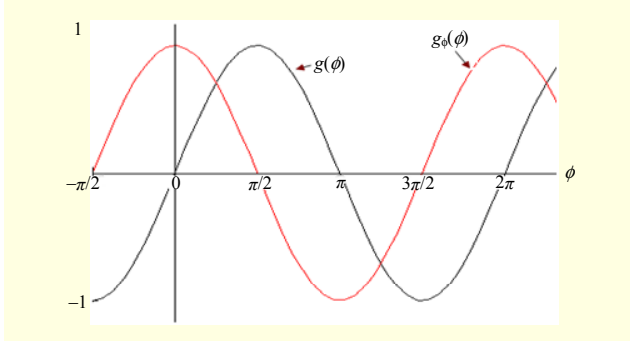


Fig. 2. Sinusoidal PD output characteristic.

the PD can also be redefined as

$$\phi(t) = \theta_1(t) - \theta_2(t). \quad (9)$$

By using (8) as a substitute in (6), the control voltage can be expressed as

$$e(t) = \frac{1}{K_3} \frac{d\theta_2}{dt}. \quad (10)$$

Also, using (10) and (3) as substitutes in (5) yields

$$\frac{d}{dt} \left[\frac{1}{K_3} \frac{d\theta_2}{dt} \right] = K_2 \left[\frac{d}{dt} + a \right] K_1 g(\phi). \quad (11)$$

Now, using (9) and redefining $G \equiv K_1 K_2 K_3$ as the closed loop gain of the system, (11) can be written as

$$\frac{d}{dt} \left[\frac{d}{dt} (\phi - \theta_1) \right] = -G \left[\frac{d}{dt} + a \right] g(\phi). \quad (12)$$

By using (7), (12) can be further simplified as

$$\frac{d^2 \phi}{dt^2} + G \frac{d}{dt} g(\phi) + G a g(\phi) = 0. \quad (13)$$

Finally, by normalizing the independent variable by the closed loop gain as $\tau = tG$, the normalized system equation can be expressed as

$$\frac{d^2 \phi}{d\tau^2} + g_\phi(\phi) \frac{d\phi}{d\tau} + a' g(\phi) = 0, \quad (14)$$

where $a' = a/G$ is the normalized integrator gain and $g_\phi(\phi) \equiv \frac{d}{d\phi} g(\phi)$ [1], [2]. Figure 2 shows the PD output $g(\phi) = \sin \phi$ and its derivative $g_\phi(\phi) = \cos \phi$ for a sinusoidal PD, and, by inserting them in (14), the dynamics of a gain normalized second-order Type II PLL can be described by [1], [2], [4]:

$$\frac{d^2 \phi}{d\tau^2} + \cos \phi \frac{d\phi}{d\tau} + a' \sin \phi = 0. \quad (15)$$

This second-order nonlinear equation, like many other

nonlinear systems, does not have a closed form solution. Therefore, the phase portrait is used to analyze the behavior of this system. However, the location and the type of the equilibrium points describe the local behavior around them as long as the equilibrium points are hyperbolic. At times, this local behavior may be extended to get some idea of the global behavior of the system as well. Furthermore, because of the presence of the sinusoidal (2π -periodic) nonlinearity in the system equation, it is obvious that the phase portrait of the system will manifest similar periodicity. Thus, the phase portrait of such a system can be completely visualized by wrapping it on the surface of a cylinder of unity radius [5]. Therefore, the behavioral study of the system can be restricted in one period, sometimes also known as a cell, without the loss of generality.

It is worth mentioning that the system model derived above precludes the presence of noise at any point in the loop. Therefore, the following analysis will assume a noiseless operating environment.

III. System Dynamics in Phase Plane

To be able to take advantage of the phase plane, the nonlinear second-order (15) must be decomposed in a set of two first-order simultaneous equations as

$$\frac{d\phi}{d\tau} = \dot{\phi}, \quad (16a)$$

$$\frac{d\dot{\phi}}{d\tau} = -\dot{\phi} \cos \phi - a' \sin \phi, \quad (16b)$$

where $\dot{\phi}$ is the frequency error.

The equilibrium points for the above system can be found by equating the right-hand sides of (16) to zero, which yields

$$\dot{\phi} = 0, \quad (17)$$

$$\phi = n\pi, \quad (18)$$

where $n=0, \pm 1, \pm 2, \pm 3, \dots$. Therefore, the two equilibrium points in an arbitrary cell, defined as $\left(-\frac{\pi}{2} \leq \phi \leq \frac{3\pi}{2}\right)$, are

$$(\phi, \dot{\phi}) = (0, 0) \text{ and } (\phi, \dot{\phi}) = (\pi, 0).$$

Now, by linearizing the nonlinear system described by (16) around the first equilibrium point at $(\phi, \dot{\phi}) = (0, 0)$, the constant coefficient matrix of the corresponding linear homogeneous system can be found as

$$A_0 = \begin{bmatrix} 0 & 1 \\ -a' & -1 \end{bmatrix}.$$

The two distinct eigenvalues of this matrix can be found as

$$\lambda_{01} = \frac{1}{2}(-1 - j\sqrt{4a' - 1}), \quad (19a)$$

$$\lambda_{02} = \frac{1}{2}(-1 + j\sqrt{4a' - 1}). \quad (19b)$$

The negative real part of the complex eigenvalues indicates that the trajectories approach the equilibrium point as time approaches infinity and the imaginary part, for $a' > 1/4$, indicates the rotational feature of the trajectories. Thus, the equilibrium point at $(\phi, \dot{\phi}) = (0, 0)$ is a spiral stable node, more commonly known as a focus. Further analysis, by decomposing the (real) component vectors of the complex eigenvector associated with λ_0 into two orthogonal vectors in the phase plane, can show that the direction of rotation of the trajectories around the focus is clockwise [5]. However, for $a' \leq 1/4$, both of these eigenvalues become real negative and, therefore, the trajectories lose the spiral features and the equilibrium point turns into a regular stable node, more commonly known as a sink. According to a fundamental theory of differential equations, sometimes known as the linearization theorem, the nonlinear flow is conjugate to the flow of the linearized system in a small neighborhood of the equilibrium point as long as the equilibrium point is hyperbolic [6], [7]. Figure 4 shows a representative phase portrait for the original system, drawn with Matlab for $a' = 0.5$. Only one focus at the origin is shown in the figure, though the other foci are located to the right as well as to the left of it, each at a 2π interval.

Similarly, by linearizing the nonlinear system, described by (16), around the other equilibrium point at $(\phi, \dot{\phi}) = (\pi, 0)$, the constant coefficient matrix of the corresponding linear homogeneous system can be found as

$$A_\pi = \begin{bmatrix} 0 & 1 \\ a' & 1 \end{bmatrix}.$$

The two distinct eigenvalues of this matrix can be found as

$$\lambda_{\pi 1} = \frac{1}{2}(1 - \sqrt{4a' + 1}), \quad (20a)$$

$$\lambda_{\pi 2} = \frac{1}{2}(1 + \sqrt{4a' + 1}). \quad (20b)$$

Since the positive normalized integrator gain ($a' > 0$) implies that $\lambda_{\pi 2} > 0 > \lambda_{\pi 1}$, the equilibrium point at $(\phi, \dot{\phi}) = (\pi, 0)$ is a *saddle point* [6], [7]. Figure 3 shows the saddle point in the phase portrait of the linearized system. L1 and L2 in Fig. 3 are the eigenvectors of the constant coefficient matrix A_π . The four separatrices associated with the saddle point lie on the four half-lines, disjoint at the saddle point, denoted by L1 and L2.

These eigenvectors, which coincide with the separatrices, can be found by shifting the origin to the saddle point at

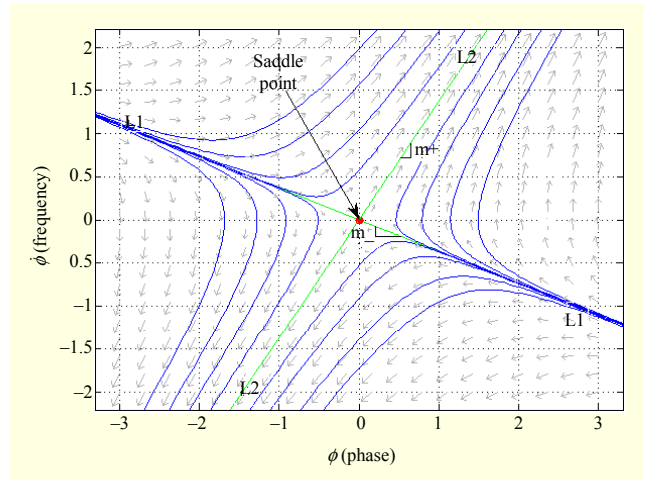


Fig. 3. Phase portrait of corresponding linearized system around saddle point, for $a' = 0.5$.

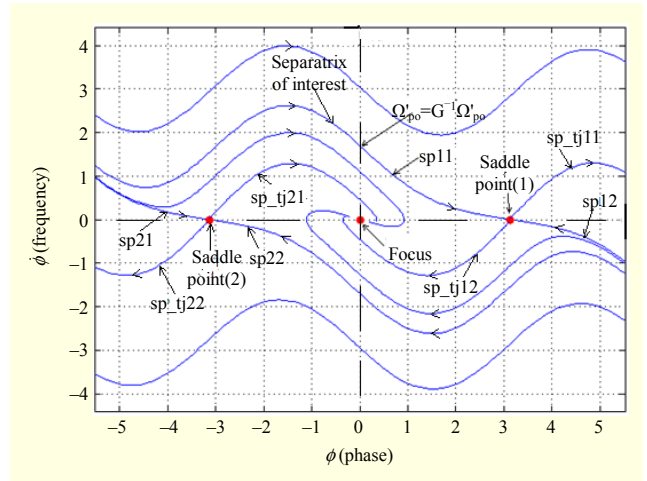


Fig. 4. Typical phase portrait of second-order Type II PLL employing sinusoidal PD.

$(\phi, \dot{\phi}) = (\pi, 0)$. Thus, it can be shown that the two half-line separatrices (stable lines) that approach the saddle point as time approaches infinity, residing on the eigenvector L1, has a slope of

$$m_- = \frac{1}{2}(1 - \sqrt{4a' + 1}). \quad (21a)$$

For $a' > 0$, m_- is negative and this eigenvector is tangent to the trajectories sp11 and sp12 of the original nonlinear system, at the saddle point, as shown in Fig. 4. Here in the naming convention of the trajectories, the first subscript identifies one of the two saddle points shown in the figure and the second subscript distinguishes between the upper and lower half-planes. Interestingly, the above-mentioned trajectories, namely, sp11 and sp12, remain as separatrices even in the nonlinear system. Thus, any solution of the original nonlinear system that starts below sp11 (alternatively, above sp12) will approach the

focus at the origin (alternatively, the focus at $(\phi, \dot{\phi}) = (2\pi, 0)$). On the other hand, any solution that starts above sp11 (alternatively, below sp12) will approach one of the foci located at every 2π interval to the right of the focus at the origin (alternatively, to the left of the focus at $(\phi, \dot{\phi}) = (2\pi, 0)$), giving rise to an event called cycle(s) slip in the PLL literature. Similar is true for the pair of separatrices sp21 and sp22, associated with the second saddle point shown in Fig. 4, located at $(\phi, \dot{\phi}) = (-\pi, 0)$ and so on.

Likewise, it can be shown that the two half-line separatrices (unstable lines), which move away from the saddle point as time approaches infinity, residing on the eigenvector L2 have a slope of

$$m_+ = \frac{1}{2}(1 + \sqrt{4a' + 1}). \quad (21b)$$

For $a' > 0$, m_+ is positive and this eigenvector is tangent to the trajectories sp_tj11 and sp_tj12 of the original nonlinear system, at the saddle point, as shown in Fig. 4. However, the above-mentioned trajectories, namely, sp_tj11 and sp_tj12, do not remain as separatrices (unstable) for the nonlinear system outside the small neighborhood around the saddle point at $(\phi, \dot{\phi}) = (\pi, 0)$. The trajectory sp_tj11 approaches the focus at $(\phi, \dot{\phi}) = (2\pi, 0)$ and the other trajectory sp_tj12 approaches the focus at the origin, as time approaches infinity, as shown in Fig. 4. This phenomenon is known as the hangup [8]. Similar is true for the saddle points in every other cell in the phase portrait.

In summary, as time approaches infinity, any initial point on the phase plane approaches one of the foci, except for those that lie on one of the separatrices, for example, sp11, sp12, sp21, sp22, and so on, as shown in Fig. 4. In other words, for a second-order Type II PLL, the foci are the global attracting points for the entire phase plane, except for the points residing on the separatrices. Thus, the entire phase plane becomes the pull-in range for such PLLs, which is indeed a very attractive feature [1]. It is also interesting to notice the symmetry of the phase portrait shown in Fig. 4 for such a system. In other words, a trajectory remains a trajectory when both ϕ -axis and $\dot{\phi}$ -axis are negated [7].

IV. Pull-Out Frequency

The pull-out frequency is defined as the maximum value of the input reference frequency step that can be applied to a phase-locked PLL, yet the loop is able to relock without slipping a cycle. In light of the phase portrait, it can be defined as the frequency axis intercept by the *separatrix*. Given the symmetry of the phase portrait mentioned above, both the upper and the lower half-planes would generate the same result.

For the frequency modulated systems, in particular, this specific parameter may dictate the allowable band for frequency swing or vice versa. It is important to note here that the notion of pull-out frequency, as it is defined for a Type II PLL, has not been generalized to the case of a Type I PLL. In fact, such a generalization may not be possible since phase plane structure for a Type I PLL generally changes with variations in $\omega_\Delta = \omega_i - \omega_0$, the loop detuning parameter. As ω_Δ changes, equilibrium point locations change, and bifurcations can occur [1], [2], [4].

V. Derivation of Formula to Approximate Pull-Out Frequency

For convenience, by substituting $\phi = x$ and $\dot{\phi} = y$ in (16), we get

$$\frac{dy}{dx} = -\cos x - a' \frac{\sin x}{y}. \quad (22)$$

The intent here is to find the intercept of the y -axis, $\dot{\phi}$ -axis in Fig. 4, by the separatrix. Therefore, integrating (22) in that range produces

$$\int_0^\pi \frac{dy}{dx} dx = \int_0^\pi -\cos x dx - a' \int_0^\pi \frac{\sin x}{y} dx. \quad (23)$$

We know from section II that $\dot{\phi}(\pi) = y(\pi) = 0$. Substituting this in the above equation yields

$$y(0) = a' \int_0^\pi \frac{\sin x}{y} dx. \quad (24)$$

Since the integral on the right-hand side does not have a closed-form solution, we must resort to an approximation technique to calculate it.

Let us expand the function $y(x)$ around the saddle point at $x = \pi$ in an asymptotic series, also known as the Poincaré expansion [9], as

$$y(x) = y(\pi) + \frac{y'(\pi)}{1!}(x - \pi) + \frac{y''(\pi)}{2!}(x - \pi)^2 + \frac{y'''(\pi)}{3!}(x - \pi)^3 + \dots \quad (25)$$

Substituting $y(\pi) = 0$ and redefining $k_1 \equiv \frac{y'(\pi)}{1!} = \frac{1}{1!} \frac{dy}{dx} \Big|_{x=\pi}$, $k_2 \equiv \frac{y''(\pi)}{2!} = \frac{1}{2!} \frac{d^2y}{dx^2} \Big|_{x=\pi}$, $k_3 \equiv \frac{y'''(\pi)}{3!} = \frac{1}{3!} \frac{d^3y}{dx^3} \Big|_{x=\pi}$, and so on, (25) can be rewritten as

$$y(x) = k_1(x - \pi) + k_2(x - \pi)^2 + k_3(x - \pi)^3 + \dots \quad (26)$$

Differentiating both sides with respect to x yields

$$\frac{dy}{dx} = k_1 + 2k_2(x-\pi) + 3k_3(x-\pi)^2 + 4k_4(x-\pi)^3 + \dots \quad (27)$$

Likewise, the two trigonometric functions $\cos x$ and $\sin x$ can also be expanded, respectively, around the same point, using the Taylor series as

$$\begin{aligned} \cos(x) = & \cos(\pi) - \frac{\sin(\pi)}{1!}(x-\pi) - \frac{\cos(\pi)}{2!}(x-\pi)^2 \\ & + \frac{\sin(\pi)}{3!}(x-\pi)^3 + \dots \end{aligned} \quad (28)$$

and

$$\begin{aligned} \sin(x) = & \sin(\pi) + \frac{\cos(\pi)}{1!}(x-\pi) - \frac{\sin(\pi)}{2!}(x-\pi)^2 \\ & - \frac{\cos(\pi)}{3!}(x-\pi)^3 + \dots \end{aligned} \quad (29)$$

Using (26)-(29) as substitutes in (22) gives

$$\begin{aligned} & k_1 + 2k_2(x-\pi) + 3k_3(x-\pi)^2 + 4k_4(x-\pi)^3 + \dots \\ = & - \left[\cos(\pi) - \frac{\sin(\pi)}{1!}(x-\pi) - \frac{\cos(\pi)}{2!}(x-\pi)^2 \right. \\ & \left. + \frac{\sin(\pi)}{3!}(x-\pi)^3 + \dots \right] \\ & - a' \frac{\sin(\pi) + \frac{\cos(\pi)}{1!}(x-\pi) - \frac{\sin(\pi)}{2!}(x-\pi)^2 - \dots}{k_1(x-\pi) + k_2(x-\pi)^2 + k_3(x-\pi)^3 + \dots} \end{aligned} \quad (30)$$

After cross multiplying and rearranging, (30) becomes

$$\begin{aligned} & [k_1 + 2k_2(x-\pi) + 3k_3(x-\pi)^2 + 4k_4(x-\pi)^3 + \dots][k_1(x-\pi) \\ & + k_2(x-\pi)^2 + k_3(x-\pi)^3 + \dots] \\ = & \left[1 - \frac{1}{2}(x-\pi)^2 + \dots \right] [k_1(x-\pi) + k_2(x-\pi)^2 + k_3(x-\pi)^3 + \dots] \\ & + a' \left[(x-\pi) - \frac{1}{6}(x-\pi)^3 + \dots \right] \end{aligned} \quad (31)$$

Now, equating the coefficients of $(x-\pi)$ from both sides of (31) yields

$$\begin{aligned} & k_1^2 = k_1 + a' \\ \Rightarrow & k_1^2 - k_1 - a' = 0 \\ \Rightarrow & k_1 = \frac{1}{2}(1 \pm \sqrt{4a'+1}). \end{aligned} \quad (32)$$

As mentioned in section III, the separatrix of interest has a negative slope (m_-) at the saddle point $(\phi, \dot{\phi}) \equiv (x, y) = (\pi, 0)$, and it is that slope according to the definition of k_1 . Therefore, the value to keep is

$$k_1 \equiv m_- = \frac{1}{2}(1 - \sqrt{4a'+1}). \quad (33)$$

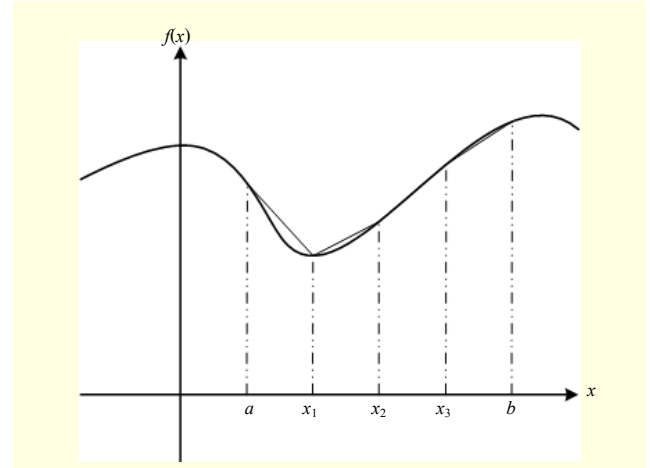


Fig. 5. Four-interval Simpson's rule to approximate integrals.

Equating the coefficients of $(x-\pi)^2$ from both sides of (31) yields

$$\begin{aligned} & k_1 k_2 + 2k_1 k_2 = k_2 \\ \Rightarrow & k_2(3k_1 - 1) = 0. \end{aligned} \quad (34)$$

Since negative k_1 implies that $k_1 \neq \frac{1}{3}$, therefore, $k_2 = 0$.

Equating the coefficients of $(x-\pi)^3$ from both sides of (31) yields

$$k_1 k_3 + 2k_2^2 + 3k_1 k_3 = k_3 - \frac{k_1}{2} - \frac{a'}{6}. \quad (35)$$

After inserting $k_2=0$ and simplifying the above equation, k_3 can be expressed as

$$k_3 = \frac{a' + 3k_1}{6(1 - 4k_1)}. \quad (36)$$

Thus, the function $y(x)$ can be approximated by the first three terms in (26) as

$$y(x) \approx k_1(x-\pi) + \frac{a' + 3k_1}{6(1 - 4k_1)}(x-\pi)^3, \quad (37)$$

where k_1 is given in (33).

Now, we are ready to approximate the integral in (24) using the four-interval Simpson's rule, which says

$$\int_a^b f(x) \approx \frac{h}{3}[f(a) + 4f(x_1) + 2f(x_2) + 4f(x_3) + f(b)], \quad (38)$$

where, $h = (b-a)/4$, $x_1 = a + h$, $x_2 = a + 2h$, and $x_3 = a + 3h$, as shown in Fig. 5 [10]. In our case, $x = \frac{\sin(x)}{y(x)}$, $a = 0$, $b = \pi$,

$x_1 = \pi/4$, $x_2 = 2\pi/4$, and $x_3 = 3\pi/4$.

Substituting these and using (37) in (38), we get

$$y(0) \approx a' \frac{\pi}{12} \left[\frac{\sin(0)}{y(0)} + \frac{4 \sin\left(\frac{\pi}{4}\right)}{k_1 \left(-\frac{3\pi}{4}\right) + \frac{a' + 3k_1}{6(1-4k_1)} \left(-\frac{3\pi}{4}\right)^3} + \frac{2 \sin\left(\frac{2\pi}{4}\right)}{k_1 \left(-\frac{2\pi}{4}\right) + \frac{a' + 3k_1}{6(1-4k_1)} \left(-\frac{2\pi}{4}\right)^3} + \frac{4 \sin\left(\frac{3\pi}{4}\right)}{k_1 \left(-\frac{\pi}{4}\right) + \frac{a' + 3k_1}{6(1-4k_1)} \left(-\frac{\pi}{4}\right)^3} + \frac{\sin(\pi)}{y(\pi)} \right] \quad (39)$$

Now, the non-zero pull-out frequency implies that $\dot{\phi}(0) = y(0) \neq 0$. Therefore, the first term in (39) drops out. The last term $\frac{\sin(\pi)}{y(\pi)}$ is in $\frac{0}{0}$ form. Applying L'Hospital's rule, its limiting value at $x = \pi^-$ can be evaluated as

$$\frac{\cos(\pi^-)}{y'(\pi^-)} = \frac{-1}{k_1}. \quad (40)$$

Thus, the pull-out frequency can be expressed as

$$\Omega'_{po} = \dot{\phi}(0) = y(0) \approx -a' \frac{\pi}{12} \left[\frac{4 \sin\left(\frac{\pi}{4}\right)}{k_1 \left(\frac{3\pi}{4}\right) + \frac{a' + 3k_1}{6(1-4k_1)} \left(\frac{3\pi}{4}\right)^3} + \frac{2 \sin\left(\frac{2\pi}{4}\right)}{k_1 \left(\frac{2\pi}{4}\right) + \frac{a' + 3k_1}{6(1-4k_1)} \left(\frac{2\pi}{4}\right)^3} + \frac{4 \sin\left(\frac{3\pi}{4}\right)}{k_1 \left(\frac{\pi}{4}\right) + \frac{a' + 3k_1}{6(1-4k_1)} \left(\frac{\pi}{4}\right)^3} + \frac{1}{k_1} \right], \quad (41)$$

where k_1 is given in (33).

It is to be noted here that the pull-out frequency in (41) is normalized by the system closed loop gain G , as shown in Fig. 4. Therefore, it must be multiplied by G to obtain the absolute value of the pull-out frequency.

VI. Comparison between Derived and Existing Empirical Formula

As mentioned in section I, Viterbi empirically derived a formula to calculate the pull-out frequency of a second-order PLL employing a sinusoidal PD, which is [1], [2]

$$\Omega'_{po} = 1.85(0.5 + \sqrt{a'}).$$

However, in the literature, no analytical approach has been found to derive a formula for Ω'_{po} . Table 1 shows the comparison of the gain normalized pull-out frequency for the entire practical range of a' , calculated using three different methods. The second column represents the numerically calculated values of the pull-out frequency using Matlab. A

Table 1. Comparison of pull-out frequency from three different methods.

a'	Numerical simulation	Empirical formula	%err (EF*)	Derived formula	%err (DF**)
0.1	1.474	1.469	0.325	1.567	6.275
0.2	1.725	1.705	1.159	1.753	1.606
0.3	1.883	1.886	0.154	1.913	1.604
0.35	1.976	1.965	0.562	1.987	0.541
0.4	2.052	2.038	0.662	2.057	0.224
0.5	2.181	2.173	0.376	2.187	0.284
0.6	2.313	2.294	0.808	2.308	0.216
0.7	2.418	2.406	0.496	2.421	0.120
0.8	2.542	2.51	1.259	2.527	0.582
0.9	2.638	2.608	1.152	2.628	0.375
1.0	2.743	2.7	1.567	2.724	0.685
1.1	2.850	2.788	2.179	2.816	1.182
1.2	2.927	2.872	1.885	2.905	0.765
1.3	3.021	2.952	2.274	2.99	1.032
1.4	3.091	3.03	1.979	3.072	0.614
1.5	3.220	3.105	2.984	3.152	1.509
1.6	3.251	3.177	2.282	3.229	0.680
1.7	3.339	3.247	2.758	3.304	1.051
1.8	3.421	3.315	3.098	3.377	1.286
1.9	3.493	3.381	3.203	3.448	1.282
2.0	3.570	3.446	3.485	3.518	1.468

*% error when results from empirical formula compared with numerical results

**% error when results from derived formula compared with numerical results

detailed procedure for a numerical approximation technique can be found in [11]. The third column denotes the value calculated using the empirical formula described by (32). The fourth column shows the percentage error when the values calculated using the empirical formula is compared with the simulation results. The fifth column displays the value calculated by the derived formula described by (31), whereas the last column lists the percentage error when these values are compared with the simulation results.

VII. Conclusion

It is evident from Table 1 that the derived formula outperforms the empirical formula for $a' \geq 0.35$ and that the percentage error when compared against the simulated results is less than 1.5%. For very low values of the loop parameter, $a' < 0.35$, the empirical formula calculates the normalized pull-out frequency with better accuracy, though such values of a' are rare in practice and only found in the applications in which

jitter tolerance is extremely tight. For such low values of normalized integrator gain (a'), the contribution from the third-order term (k_3) in the asymptotic series becomes insignificant and the integral approximation from the four-interval Simpson's rule becomes coarse and thus contribute to the poor performance of the derived formula.

In the PLL design practice, $a'=0.5$ is a standard starting value for normalized integrator gain. This comes from the damping coefficient $\zeta=0.707$, the most commonly used value in the linear control systems, which offers a satisfactory trade-off between the overshoot and the settling time. It is also to be noted here that the linear model of the PLL is not adequate when the absolute value of the phase error grows beyond 30° . Most commonly used values for the normalized integrator gain stay within 0.5 to 1.5 to accommodate a larger phase error.

The improvement achieved from the new formula is significant for the high gain (G) systems, when the gain normalized pull-out frequency is multiplied by G to calculate its absolute value. For instance, the percentage error when using the empirical formula and the derived formula to calculate the gain normalized pull-out frequency, for the normalized integrator gain $a'=1.0$, are 1.152% and 0.685%, respectively. However, the improvement gained from the derived formula when compared with the empirical one is $[(1.152 - 0.685) / 1.152] \times 100\% = 40\%$. Thus, in the case of large closed loop gain ($G > 10$), the improvement achieved by using the derived formula is significant when calculating the absolute value of the pull-out frequency. Though the derived formula may look overly complicated as opposed to the empirical one, it can still be computed easily by using a modern scientific calculator and is still worth the improvement. The formula may as well be computed easily at the Matlab command prompt.

References

- [1] F.M. Gardner, *Phaselock Techniques*, 2nd ed., New York: Wiley-Interscience, 1979.
- [2] J.L. Stensby, *Phase-Locked Loops: Theory and Applications*, Boca Raton, FL: CRC Press, 1997.
- [3] A.-S. Huque and J.L. Stensby, "An Exact Formula for the Pull-Out Frequency of a 2nd-Order Type II Phase Lock Loop," *IEEE Commun. Lett.*, vol. 15, no. 12, Dec. 2011, pp. 1384-1387.
- [4] W.F. Egan, *Phase-Lock Basics*, Hoboken, NJ: Wiley-Interscience, 1998.
- [5] A.A. Andronov, A.A. Vitt, and S.E. Khaik, *Theory of Oscillators*, 2nd ed., Mineola, NY: Dover Publications, 1987.
- [6] M.W. Hirsch, S. Smale, and R.L. Devaney, *Differential Equations, Dynamical Systems & An Introduction to Chaos*, 2nd ed., San Diego, CA: Elsevier Academic Press, 2004.
- [7] L. Perko, *Differential Equations and Dynamical Systems*, 3rd ed., Berlin, Germany: Springer-Verlag, 1991.
- [8] F.M. Gardner, "Hangup in Phase-Lock Loops," *IEEE Trans. Commun.*, vol. COM-25, no. 10, Oct. 1977, pp. 1210-1214.
- [9] A. Erdelyi, *Asymptotic Expansions*, Mineola, NY: Dover Publications, 1956.
- [10] F.B. Hildebrand, *Introduction to Numerical Analysis*, 2nd ed., Mineola, NY: Dover Publications, 1974.
- [11] J. Stensby, "An Approximation of the Pull-Out Frequency Parameter in a Second-Order PLL," *Proc. 38th Southeastern Symp. Syst. Theory*, 2006, pp. 75-79.



Abu-Sayeed Huque received his BSc from Bangladesh University of Engineering and Technology, Dhaka, Bangladesh, in 1996 and MSE from the University of Texas at Arlington, Arlington, TX, USA, in 1997 in electrical engineering. He joined Qualcomm Inc., San Diego, CA, USA, in 1998, where he was involved in the digital design of CDMA-based phones, base-station channel cards, chipsets, and so on, until he resigned in 2008 to go back to school. He received his PhD from the University of Alabama in Huntsville, Huntsville, AL, USA, in 2011. He taught in Oakwood University and University of Alabama in Huntsville. Currently, he is with the University of Tabuk, Saudi Arabia, as an assistant professor in the department of electrical engineering. His research interest includes synchronization, radar communications, mathematical modeling, and smart grids.



John Stensby received his BSEE from the University of Alabama, Tuscaloosa, AL, USA, in 1972, his MSE from the University of Alabama in Huntsville, Huntsville, AL, USA, in 1976, and his PhD from Texas A&M University, College Station, TX, USA, in 1981. Previously, he worked for Rockwell International (Anaheim, CA, USA), Texas Instruments (Dallas, TX, USA), and the University of Kansas (Lawrence, KS, USA). Since 1984, he has been employed by the University of Alabama in Huntsville, where he currently serves as a full professor of electrical and computer engineering. His research interests include communication and control theory, applied mathematics, and numerical analysis.